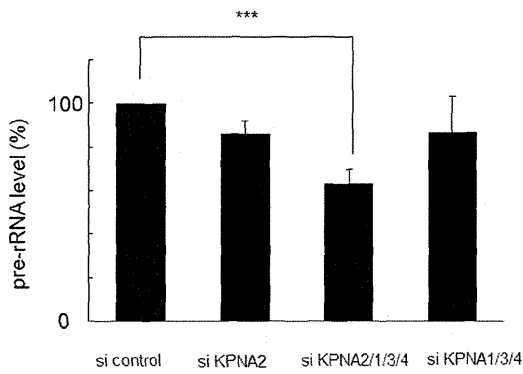


**Table 1. Cont.**

<b>mRNA processing</b>	
ING5	Inhibitor of growth protein 5
RBBP4	Histone-binding protein RBBP4
RBBP7	Histone-binding protein RBBP7
ARID2	AT-rich interactive domain-containing protein 2
CHD8	Chromodomain-helicase-DNA-binding protein 8
HDAC2	Histone deacetylase 2
HDAC1	Histone deacetylase 1
ASH1L	Probable histone-lysine N-methyltransferase ASH1L
BRDT	Bromodomain testis-specific protein
RBM14	RNA-binding protein 14
BCOR	BCL-6 corepressor
CHD4	Chromodomain-helicase-DNA-binding protein 4
MLL2	Histone-lysine N-methyltransferase MLL2
<b>Nucleocytoplasmic transport</b>	
PHAX	Phosphorylated adapter RNA export protein
NCBP1	Nuclear cap-binding protein subunit 1
UPF1	Regulator of nonsense transcripts 1
SET	Protein SET
GLE1	Nucleoporin GLE1
NUPL2	Nucleoporin-like protein 2
TPR	Nucleoprotein
KPNA2	Importin subunit alpha-2
KPNB1	Importin subunit beta-1
BAT1	Spliceosome RNA helicase BAT1
<b>Transcription</b>	
ING5	Inhibitor of growth protein 5
NMI	N-myc-interactor
FOXK1	Forkhead box protein K1
FOXM1	Forkhead box protein M1
CCNT1	Cyclin-T1
ARID2	AT-rich interactive domain-containing protein 2
YBX1	Nuclease-sensitive element-binding protein 1
CNOT4	CCR4-NOT transcription complex subunit 4
YBX2	Y-box-binding protein 2
CHD8	Chromodomain-helicase-DNA-binding protein 8
ASH2L	Set1/Ash2 histone methyltransferase complex subunit ASH2
BCOR	BCL-6 corepressor
EWSR1	RNA-binding protein EWS
CHD4	Chromodomain-helicase-DNA-binding protein 4
MLL2	Histone-lysine N-methyltransferase MLL2
ASXL3	Putative Polycomb group protein ASXL3
TAF4	Transcription initiation factor TFIID subunit 4
RBBP4	Histone-binding protein RBBP4
TAF6	Transcription initiation factor TFIID subunit 6
POLR1A	DNA-directed RNA polymerase I subunit RPA1
MED12	Mediator of RNA polymerase II transcription subunit 12
CSDA	DNA-binding protein A

doi:10.1371/journal.pone.0076416.t001



**Figure 4. Suppression of ribosomal RNA synthesis by combined KPNA knockdown.** Under starvation conditions (0.1% fetal bovine serum), siRNA-mediated knockdown of KPNA2, 1, 3, and 4 significantly suppressed ribosomal RNA synthesis analyzed by reverse transcription-quantitative polymerase chain reaction (\*\* $p < 0.01$ ). The amount of pre-ribosomal RNA was reduced by about 37% after 72 h. doi:10.1371/journal.pone.0076416.g004

by SDS-PAGE, and silver stained. HaCaT cells expressing GFP-TAP were used as a negative control (Figure 3a). KPNA2-TAP-associated proteins extracted from the silver-stained gel were identified by mass spectrometry. Numerous proteins were analyzed by reactome (<http://www.reactome.org>) to investigate their biological relationships. Pathway analysis revealed that the proteins interacting with KPNA2 were associated with mRNA processing, ribonucleoprotein complex biogenesis, chromatin modification, and transcription, all of which are essential for cell activities including cell growth (Figure 3b, Table 1). Interestingly, significant numbers of ribosomal proteins were listed as associated with KPNA2. Furthermore, immunofluorescence staining of KPNA2 in cultured HaCaT keratinocytes demonstrated co-localization of KPNA2 with UBF in the nucleoli, suggesting a role of KPNA2 for maintaining rRNA function (Figure 3c).

**Contribution of KPNA2 to Protein Synthesis and Ribosomal RNA Transcription**

Because the nucleolus is specifically responsible for rRNA transcription and maintenance of gene expression/transcription

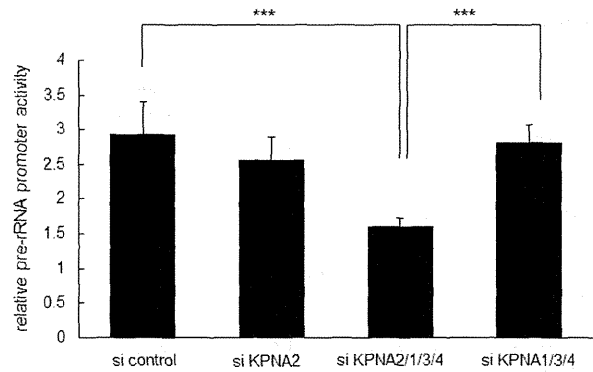


**Figure 6. Suppression of the pre-ribosomal RNA promoter by combined KPNA knockdown.** Under starvation conditions (0.1% fetal bovine serum), siRNA-mediated knockdown of KPNA2, 1, 3, and 4 significantly suppressed pre-rRNA promoter activity after 24 h (\*\* $p < 0.01$ ). doi:10.1371/journal.pone.0076416.g006

and mRNA processing, we hypothesized that KPNA2 in the nucleoli may regulate rRNA transcription to maintain cell growth under starvation conditions. To test this hypothesis, the siRNA cocktail was again applied to knockdown KPNA2 to observe the effect on pre-rRNA transcription in starved HaCaT keratinocytes. Knockdown of all KPNA2 reduced pre-rRNA levels as measured by RT-qPCR. In the 72 h after treatment with the siRNA cocktail, pre-rRNA expression was reduced by about 40%. Subtraction of KPNA2 siRNA restored pre-rRNA expression. The other KPNA2 did not contribute to pre-rRNA expression. Treatment with KPNA2 siRNA alone had no significant effect, suggesting a redundant mechanism with other KPNA2 (Figure 4). Protein synthesis in HaCaT keratinocytes was also reduced, corresponding to the suppression of pre-rRNA expression (Figure 5). The pre-rRNA promoter was also suppressed by KPNA2 knockdown after 24 h (Figure 6). Fluorescence-activated cell sorting of HaCaT cells before and after KPNA2 knockdown showed no significant change in the cell cycle pattern (data not shown). These data suggest KPNA2 might positively regulate rRNA transcription in the nucleolus, maintaining cell growth by ensuring transcription and translation directly or indirectly.

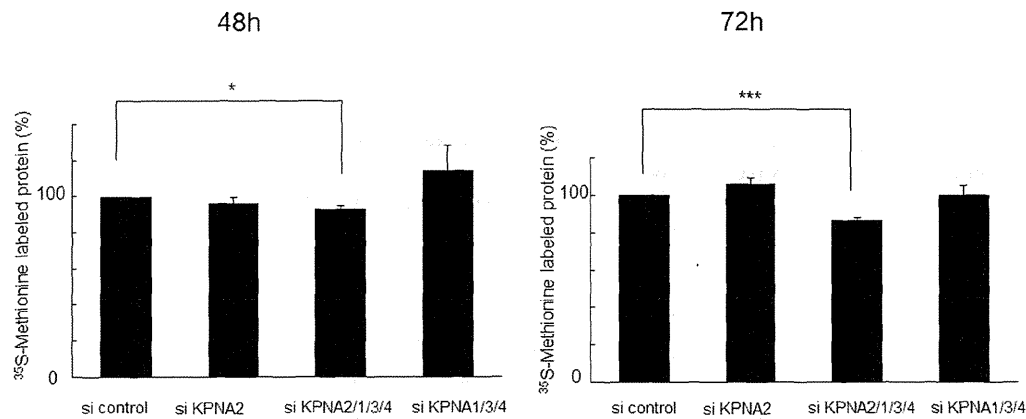


**Figure 5. Suppression of protein synthesis by combined KPNA knockdown.** Under starvation conditions (0.1% fetal bovine serum), siRNA-mediated knockdown of KPNA2, 1, 3, and 4 significantly suppressed protein synthesis after 48 h (\* $p < 0.05$ ) and 72 h (\*\* $p < 0.01$ ), as demonstrated by metabolic labeling with <sup>35</sup>S-methionine. doi:10.1371/journal.pone.0076416.g005

## Discussion

In this study, KPNA2 was overexpressed in proliferating disorders of the skin and interacted with many kinds of proteins that control transcription and gene expression directly and indirectly. This was the first report to show that KPNA2 is essential for cell growth in terms of rRNA and protein synthesis under starvation conditions.

KPNA2 overexpression in several skin malignancies is associated with varying prognoses. In the basal cells of psoriasis, KPNA2 expression was diffusely up-regulated in comparison to atopic dermatitis. Thus, KPNA2 expression might be induced in cells in which proliferation has been activated. Comparing Bowen's disease and actinic keratosis, which are known as SCC *in situ*, KPNA2 was remarkably and diffusely overexpressed. KPNA2 may therefore be a tumor marker with utility as a prognostic factor of proliferative activity in skin malignancies, although we have insufficient sample sizes to determine significance. Previous reports have demonstrated KPNA2 overexpression in various tumors cells *in vitro* and *in vivo*; elevated KPNA2 and KPNB1 expression in cancer cells correlates with altered transcriptional regulation associated with deregulated E2F/Rb activities [26]. Some studies have indicated that higher KPNA2 expression in tumor cell nuclei shortens patient survival, although the mechanisms and precise roles of KPNA2 in the tumor cells remained unclear [16,17]. Researchers also hypothesized that KPNA2-mediated nuclear transport of proteins necessary for maintaining cell proliferation, such as transcription factors, promote tumor cell growth. In this context, KPNA2 was shown to interact with NBS1 (Nijmegen breakage syndrome 1), a key regulator of the MRE11/RAD50/NBS1 complex. NBS1 promotes tumorigenesis by binding and activating the phosphatidylinositol 3-kinase/AKT pathway [27]. Interestingly, siRNA-mediated KPNA2 knockdown studies revealed a different cellular response to KPNA2 inhibition in prostate and cervical cancer cell lines. In prostate cell line PC3, proliferation and viability were significantly reduced when KPNA2 expression was inhibited, whereas there was no significant change in a cervical cancer cell line. This difference could be due to tissue-specific tumor etiologies [13,17].

In this study, we characterized KPNA2-binding proteins *in situ* in immortalized HaCaT keratinocytes. *In silico* gene ontology indicated a significant relationship between KPNA2 binding proteins and mRNA processing, ribonucleoprotein complex biogenesis, chromatin modification, and transcription. KPNA2 interacted with various ribosomal proteins and heterogeneous nuclear ribonucleoproteins directly or indirectly and was located in the nucleolus, the site of pre-rRNA transcription and processing and ribosome assembly. rRNA synthesis, the first event in ribosome synthesis, is a fundamental determinant of a cell's capacity to grow and proliferate. Ribosomal RNA genes (rDNAs) are transcribed with high efficiency and the complex regulation of rRNA synthesis is responsive to general metabolism and specific environmental challenges [20,28]. Serum starvation is also a well-

established approach to inducing a broad range of cellular stress. TAP analysis revealed that KPNA2 associates with numerous ribosomal RNA synthesis-related proteins including RNA polymerase I subunit, rRNA methyl transferase, rRNA subunit biogenesis protein, and rRNA processing proteins. Furthermore, KPNA2 accumulates in the nucleolus and contributes to rRNA transcription *in vitro*. These lines of evidence suggest KPNA2 may serve important roles as a canonical nuclear transporter and to ensure rRNA biogenesis in proliferating cells. In this context, enhanced KPNA2 expression in malignant and inflammatory keratinocytes may positively regulate their proliferating capacity by supporting rRNA synthesis, which is indispensable. In malignant cells, the poor prognosis indicated by nuclear KPNA2 accumulation may be associated with KPNA2 retention in response to cellular stress and increasing rRNA synthesis or changing gene expression.

KPNA subtypes exhibit different abilities to interact with specific NLS-containing cargos and in various expression patterns in cells and tissues. KPNA2 is highly expressed in undifferentiated embryonic stem cells and down-regulated during neural differentiation, indicating that proper expression of KPNA2 is required for embryonic stem cells to maintain their undifferentiated state [29]. KPNA2s are also complementary because they are indispensable for cellular proliferation and differentiation. We previously examined the effect of KPNA2 siRNA subtraction on RNA expression in normal human keratinocytes by microarray analysis [4]; however, there was no increase of more than 2 fold in any other KPNA2s including KPNA1, 3, 4, and KPNB1 (data not shown).

In this study, KPNA2 was essential for cell growth related to rRNA and protein synthesis under starvation conditions; however, there was no significant change when only KPNA2 was knocked down. Combined knockdown of KPNA2, 1, 3, and 4 was needed to suppress cell growth and KPNA2 was indispensable. Even under these conditions, growth suppression was gradual and mild over 120 h. Furthermore, combined knockdown of KPNA2s mildly suppressed the synthesis of rRNA and proteins after 72 h. These results indicated that KPNA2s might play complementary roles with sufficient reserves.

Further studies are needed to clarify the additional function of KPNA2 in cell proliferation, which would be a focus for a new treatment to regulate KPNA2.

## Acknowledgments

We sincerely appreciate the kind support of Prof. Yasufumi Kaneda. We also thank Ms. Eriko Nobuyoshi and Ms. Sayaka Matsumura for technical support with immunohistochemistry and reverse transcription-quantitative polymerase chain reaction.

## Author Contributions

Conceived and designed the experiments: NU KT KN TN. Performed the experiments: NU SS. Analyzed the data: NU KT KN TN IK. Contributed reagents/materials/analysis tools: HN IK. Wrote the paper: NU KT.

## References

- Pemberton LF, Paschal BM (2005) Mechanisms of receptor-mediated nuclear import and nuclear export. *Traffic* 6: 187–198.
- Yasuhara N, Oka M, Yoneda Y (2009) The role of the nuclear transport system in cell differentiation. *Semin Cell Dev Biol* 20: 590–599.
- Yasuda Y, Miyamoto Y, Yamashiro T, Asally M, Masui A, et al. (2012) Nuclear retention of importin alpha coordinates cell fate through changes in gene expression. *EMBO J* 31: 83–94.
- Umegaki N, Tamai K, Nakano H, Moritsugu R, Yamazaki T, et al. (2007) Differential regulation of karyopherin alpha 2 expression by TGF-beta1 and IFN-gamma in normal human epidermal keratinocytes: evident contribution of KPNA2 for nuclear translocation of IRF-1. *J Invest Dermatol* 127: 1456–1464.
- Freire J, Covelo G, Sarandeses C, Diaz-Jullien C, Freire M (2001) Identification of nuclear-import and cell-cycle regulatory proteins that bind to prothymosin alpha. *Biochem Cell Biol* 79: 123–131.
- Hall MN, Griffin CA, Simionescu A, Corbett AH, Pavlath GK (2011) Distinct roles for classical nuclear import receptors in the growth of multinucleated muscle cells. *Dev Biol* 357: 248–258.
- Schatz CA, Santarella R, Hoenger A, Karsenti E, Mattaj JW, et al. (2003) Importin alpha-regulated nucleation of microtubules by TPX2. *EMBO J* 22: 2060–2070.

8. Gruss OJ, Carazo-Salas RE, Schatz CA, Guarguaglini G, Kast J, et al. (2001) Ran induces spindle assembly by reversing the inhibitory effect of importin alpha on TPX2 activity. *Cell* 104: 83–93.
9. Ems-McClung SC, Zheng Y, Walczak CE (2004) Importin alpha/beta and Ran-GTP regulate XCTK2 microtubule binding through a bipartite nuclear localization signal. *Mol Biol Cell* 15: 46–57.
10. Askjaer P, Galy V, Hammak E, Mattaj JW (2002) Ran GTPase cycle and importins alpha and beta are essential for spindle formation and nuclear envelope assembly in living *Caenorhabditis elegans* embryos. *Mol Biol Cell* 13: 4355–4370.
11. Harel A, Forbes DJ (2004) Importin beta: conducting a much larger cellular symphony. *Mol Cell* 16: 319–330.
12. Rotem A, Gruber R, Shorer H, Shaulov L, Klein E, et al. (2009) Importin beta regulates the seeding of chromatin with initiation sites for nuclear pore assembly. *Mol Biol Cell* 20: 4031–4042.
13. van der Watt PJ, Maske CP, Hendricks DT, Parker MI, Denny L, et al. (2009) The Karyopherin proteins, Crm1 and Karyopherin beta1, are overexpressed in cervical cancer and are critical for cancer cell survival and proliferation. *Int J Cancer* 124: 1829–1840.
14. Winnepeninckx V, Lazar V, Michiels S, Dessen P, Stas M, et al. (2006) Gene expression profiling of primary cutaneous melanoma and clinical outcome. *J Natl Cancer Inst* 98: 472–482.
15. Wang CI, Wang CL, Wang CW, Chen CD, Wu CC, et al. (2011) Importin subunit alpha-2 is identified as a potential biomarker for non-small cell lung cancer by integration of the cancer cell secretome and tissue transcriptome. *Int J Cancer* 128: 2364–2372.
16. Gluz O, Wild P, Meiler R, Diallo-Danebrock R, Ting E, et al. (2008) Nuclear karyopherin alpha2 expression predicts poor survival in patients with advanced breast cancer irrespective of treatment intensity. *Int J Cancer* 123: 1433–1438.
17. Mortezaei A, Hermanns T, Seifert HH, Baumgartner MK, Provenzano M, et al. (2011) KPNA2 expression is an independent adverse predictor of biochemical recurrence after radical prostatectomy. *Clin Cancer Res* 17: 1111–1121.
18. Noetzel E, Rose M, Bornemann J, Gajewski M, Knuchel R, et al. (2012) Nuclear transport receptor karyopherin-alpha2 promotes malignant breast cancer phenotypes in vitro. *Oncogene* 31: 2101–2114.
19. Tanaka Y, Okamoto K, Teye K, Umata T, Yamagiwa N, et al. (2010) JmjC enzyme KDM2A is a regulator of rRNA transcription in response to starvation. *EMBO J* 29: 1510–1522.
20. Grummt I (2003) Life on a planet of its own: regulation of RNA polymerase I transcription in the nucleolus. *Genes Dev* 17: 1691–1702.
21. Murayama A, Ohmori K, Fujimura A, Minami H, Yasuzawa-Tanaka K, et al. (2008) Epigenetic control of rDNA loci in response to intracellular energy status. *Cell* 133: 627–639.
22. Rigaut G, Shevchenko A, Rutz B, Wilm M, Mann M, et al. (1999) A generic protein purification method for protein complex characterization and proteome exploration. *Nat Biotechnol* 17: 1030–1032.
23. Nimura K, Ura K, Shiratori H, Ikawa M, Okabe M, et al. (2009) A histone H3 lysine 36 trimethyltransferase links Nkx2-5 to Wolf-Hirschhorn syndrome. *Nature* 460: 287–291.
24. Shevchenko A, Wilm M, Vorm O, Mann M (1996) Mass spectrometric sequencing of proteins silver-stained polyacrylamide gels. *Anal Chem* 68: 850–858.
25. Ghoshal K, Majumder S, Datta J, Motiwala T, Bai S, et al. (2004) Role of human ribosomal RNA (rRNA) promoter methylation and of methyl-CpG-binding protein MBD2 in the suppression of rRNA gene expression. *J Biol Chem* 279: 6783–6793.
26. van der Watt PJ, Ngarande E, Leaner VD (2011) Overexpression of Kpnbeta1 and Kpnalpha2 importin proteins in cancer derives from deregulated E2F activity. *PLoS One* 6: e27723.
27. Teng SC, Wu KJ, Tseng SF, Wong CW, Kao L (2006) Importin KPNA2, NBS1, DNA repair and tumorigenesis. *J Mol Histol* 37: 293–299.
28. Moss T (2004) At the crossroads of growth control; making ribosomal RNA. *Curr Opin Genet Dev* 14: 210–217.
29. Yasuhara N, Shibasaki N, Tanaka S, Nagai M, Kamikawa Y, et al. (2007) Triggering neural differentiation of ES cells by subtype switching of importin-alpha. *Nat Cell Biol* 9: 72–79.





# Novel Anti-Microbial Peptide SR-0379 Accelerates Wound Healing via the PI3 Kinase/Akt/mTOR Pathway

Hideki Tomioka<sup>1,2</sup>, Hironori Nakagami<sup>3\*</sup>, Akiko Tenma<sup>2</sup>, Yoshimi Saito<sup>2</sup>, Toshihiro Kaga<sup>2</sup>, Toshihide Kanamori<sup>2</sup>, Nao Tamura<sup>2</sup>, Kazunori Tomono<sup>5</sup>, Yasufumi Kaneda<sup>4</sup>, Ryuichi Morishita<sup>1\*</sup>

**1** Department of Clinical Gene Therapy, Osaka University Graduate School of Medicine, 2-2 Yamada-oka, Suita, Osaka, Japan, **2** AnGesMG, Inc., 7-7-15 Saito Bio-Incubator, Ibaraki, Osaka, Japan, **3** Division of Vascular Medicine and Epigenetics, Osaka University United Graduate School of Child Development, 2-1 Yamada-oka, Suita, Osaka, Japan, **4** Division of Gene Therapy Science, Osaka University Graduate School of Medicine, School of Child Development, 2-1 Yamada-oka, Suita, Osaka, Japan, **5** Division of Infection Control and Prevention, Graduate School of Medicine, 2-2 Yamada-oka, Suita, Osaka, Japan

## Abstract

We developed a novel cationic antimicrobial peptide, AG30/5C, which demonstrates angiogenic properties similar to those of LL-37 or PR39. However, improvement of its stability and cost efficacy are required for clinical application. Therefore, we examined the metabolites of AG30/5C, which provided the further optimized compound, SR-0379. SR-0379 enhanced the proliferation of human dermal fibroblast cells (NHDFs) via the PI3 kinase-Akt-mTOR pathway through integrin-mediated interactions. Furthermore SR-0379 promoted the tube formation of human umbilical vein endothelial cells (HUVECs) in co-culture with NHDFs. This compound also displays antimicrobial activities against a number of bacteria, including drug-resistant microbes and fungi. We evaluated the effect of SR-0379 in two different wound-healing models in rats, the full-thickness defects under a diabetic condition and an acutely infected wound with full-thickness defects and inoculation with *Staphylococcus aureus*. Treatment with SR-0379 significantly accelerated wound healing when compared to fibroblast growth factor 2 (FGF2). The beneficial effects of SR-0379 on wound healing can be explained by enhanced angiogenesis, granulation tissue formation, proliferation of endothelial cells and fibroblasts and antimicrobial activity. These results indicate that SR-0379 may have the potential for drug development in wound repair, even under especially critical colonization conditions.

**Citation:** Tomioka H, Nakagami H, Tenma A, Saito Y, Kaga T, et al. (2014) Novel Anti-Microbial Peptide SR-0379 Accelerates Wound Healing via the PI3 Kinase/Akt/mTOR Pathway. PLoS ONE 9(3): e92597. doi:10.1371/journal.pone.0092597

**Editor:** Ganesh Chandra Jagetia, Mizoram University, India

**Received:** October 5, 2013; **Accepted:** February 24, 2014; **Published:** March 27, 2014

**Copyright:** © 2014 Tomioka et al. This is an open-access article distributed under the terms of the Creative Commons Attribution License, which permits unrestricted use, distribution, and reproduction in any medium, provided the original author and source are credited.

**Funding:** This study was supported by a Health Labour Sciences Research Grant in Japan, and partially funded by AnGes MG. No additional funding was received for this study. Hideki Tomioka, Akiko Tenma, Yoshimi Saito, Toshihiro Kaga, Toshihide Kanamori and Nao Tamura are employees of AnGes MG. The funder provided support in the form of salaries for authors, but did not have any additional role in the study design, data collection and analysis, decision to publish, or preparation of the manuscript. The specific roles of these authors are articulated in the "Author Contributions" section.

**Competing Interests:** Ryuichi Morishita is an Editorial Board Member of PLOS ONE. Ryuichi Morishita is a founder of AnGes MG, and a stockholder. AnGes MG has the following patent licenses of AG30/5C (PCT/JP2008/052020: Novel polypeptide and antibacterial agent comprising the same as active ingredient) and SR-0379 (PCT/JP2010/058838: Polypeptides and antibacterial or antiseptic use of same). Hideki Tomioka, Akiko Tenma, Yoshimi Saito, Toshihiro Kaga, Toshihide Kanamori and Nao Tamura are employees of AnGes MG. Department of clinical gene therapy is financially supported by AnGes MG, Novartis, Shionogi, Boehringer, and Rohto. Division of Vascular Medicine and Epigenetics is financially supported by Bayel. This study is partially supported by the fund of AnGes MG. There are no further patents, products in development or marketed products to declare. This does not alter the authors' adherence to all the PLoS ONE policies on sharing data and materials.

\* E-mail: nakagami@gts.med.osaka-u.ac.jp (HN); morishit@cgt.med.osaka-u.ac.jp (RM)

## Introduction

Antimicrobial peptides are produced by multicellular organisms as a defense mechanism against competing pathogenic microbes [1]. Currently, more than 1,200 antimicrobial peptides have been discovered in animals and plants [2]. In addition to their antimicrobial functions, some peptides, such as LL-37, are known to have other functions. For example, LL-37 is chemotactic for monocytes, T cells, neutrophils and mast cells and also stimulates mast cell histamine release and angiogenesis [3]. These observations have led to the development of a therapeutic concept using antimicrobial peptides as multifunctional effector molecules to prevent infection directly and to promote wound healing in various ulcers. Indeed, many researchers have tried to develop antimicrobial peptides for topical use and systemic application [4] [5]. Before these peptides can be used in clinical applications, several improvements must be made, including 1) increased

stability, 2) reduced cytotoxicity and 3) improved antimicrobial activity [6]. To improve the stability of antimicrobial peptides, converting amino acids from L to D conformations has been attempted [7]. Antimicrobial peptides are usually positively charged, between 12 and 100 amino acids in length and form amphipathic structures. The production of shorter analogs may also resolve the cost issue for clinical applications.

We previously developed an antimicrobial peptide named AG30 (angiogenic peptide 30) that contained 30 amino acids and possessed both angiogenic and antibacterial functions [8] [9]. For clinical application in the treatment of drug-resistant ulcers, we have modified AG30 to enhance its angiogenic activity, broaden its antibacterial function, enhance its stability and reduce its cost. In this study, we have demonstrated the production of a stable, shorter peptide, SR-0379, that contains twenty amino acids, including one lysine residue that has been converted to D-lysine. This peptide exhibited antimicrobial activities against a

number of bacteria, including drug-resistant bacteria, and induced the proliferation, tube formation, migration and contraction of human dermal fibroblast cells.

Treatment with SR-0379 significantly accelerated wound healing in a skin ulcer model. In the intracellular mechanism of wound healing, we focused on the PI3K/Akt/mTOR pathway. It has been reported that Akt/mTOR activation, by the ablation of Pten and Tsc1, dramatically increased epithelial cell proliferation, migration, and cutaneous wound healing, while pharmacological inhibition of mTOR with rapamycin delays wound closure [10]. Indeed, SR-0379 would activate the Akt/mTOR pathway which lead to accelerate wound healing. Further application of SR-0379 might provide a new therapeutic option to treat various ulcers, such as diabetic ulcers and severe burns.

## Results

### Design of SR-0379

For use in clinical applications, we first modified AG30 to improve its stability and reduce its cost. To perform the lead-to-drug-candidate optimization, various approaches to improve stability were evaluated. The metabolic stability of AG30/5C was evaluated by using matrix-assisted laser desorption/ionization time-of-flight mass spectrometry (MALDI-TOF MS) (Figure S1 in File S1). The major metabolites were 20 amino acids (aa), 18 aa and 17 aa, which overlap the N terminus AG30/5C and 12 aa in the middle of AG30/5C (Fig. 1A). The metabolites of AG30/5C were cleaved by endopeptidases and exopeptidase at multiple sites, with most cleavage sites present in the C-terminus. Those metabolites were synthesized (Fig. 1B), and their proliferation in HUVECs, tube formation in co-culture of HUVECs and NHDFs and antibacterial activities against *Escherichia coli*, *Pseudomonas aeruginosa* and *Staphylococcus aureus* were evaluated. Treatment with the 20-aa peptide (SR-0007) yielded significant increases in proliferation of HUVECs (Fig. 1C), whereas other metabolites did not have significant effects (data not shown). The stimulatory effects of SR-0007 were equivalent to the effects of AG30/5C (Fig. 1C). Furthermore, the treatment with SR-0007 (10 µg/ml) induced tube form in co-culture of HUVECs and NHDFs with the same level of AG30/5C (Fig. 1D). SR-0007 exhibited similar antibacterial activities against *Escherichia coli*, *Pseudomonas aeruginosa* and *Staphylococcus aureus* as AG30/5C (Table 1). These results revealed that SR-0007, which consists of 20 amino acids, is a potent candidate metabolite like AG30. However, SR-0007 was rapidly degraded by rat and human sera at 37°C (Figure 1E). Therefore, we further modified SR-0007 to improve its stability. The lysine in SR-0007 was replaced with D-form lysine, and the resulting compound was named SR-0379. As shown in Fig. 1E, the stability of SR-0379 was significantly improved, suggesting that SR-0379 might be resistant to the actions of known natural peptidases [11].

### Antibacterial activity of SR-0379 in drug-resistant/sensitive strains

We examined the antibacterial effects of AG30/5C, SR-0007 and SR-0379 against *E. coli*, *P. aeruginosa* and *S. aureus* (Table 1). Importantly, SR-0379 exhibited more potent antibacterial activity against *E. coli* compared to the original SR-0007 peptide, whereas the minimal inhibitory concentration (MIC) of SR-0379 against *P. aeruginosa* was equivalent to that of SR-0007. A number of strains were then evaluated for their sensitivities to SR-0379 (Table 2). SR-0379 demonstrated potent antibacterial activity against gram-positive and gram-negative aerobes and anaerobes. Additionally, SR-0379 exhibited antibacterial effects against fungi such as

*Candida krusei*. Notably, the antimicrobial spectrum of SR-0379 is broader than the spectra for antibiotics such as chloramphenicol or amphotericin B (Table 2) failed to exhibit an inhibitory activity against fungi or bacteria, respectively. Furthermore, we tested the antibacterial effects of SR-0379 on antibiotic-resistant/sensitive strains for use in clinical applications. Unexpectedly, SR-0379 exhibited similar inhibitory effects on various antibiotic-resistant strains, such as methicillin-resistant *S. aureus* (MRSA) and multidrug-resistant *Acinetobacter baumannii*, compared to the sensitive strains (Table 3). As antimicrobial peptide functional mechanisms are related to the disruption of the bacterial membrane [12], SR-0379 may exhibit potent antibacterial effects against other antibiotic-resistant strains.

### Cellular functions of SR-0379 and its molecular mechanisms

We investigated the effects of SR-0379 on the proliferation, migration and contraction capacity of neonatal normal human dermal fibroblasts (NHDFs) and examined the angiogenic activity of HUVECs in co-culture with NHDFs. In the proliferation assay, the treatment with SR-0379 (1, 3 and 10 µg/ml) resulted in significant increase in the proliferation of fibroblasts in a dose-dependent manner (Fig. 2A). Whereas Normal Human Epidermal Keratinocytes (NHEKs) were treated with SR-0379 (1, 3 and 10 µg/ml), SR-0379 did not affect cell proliferation (Figure S2 in File S1). Similarly, in the tube formation assay, the treatment with SR-0379 (0.5, 2.5 and 10 µg/ml) significantly induced tube formation of HUVECs in co-culture with NHDFs as angiogenic activity (Fig. 2B). In the migration assay, the treatment with SR-0379 (1 and 10 µg/ml) also resulted in significant increases in migration activity (Fig. 2C). In the fibroblast-collagen-matrix contraction assay, the treatment with SR-0379 (1, 3, 10 and 30 µg/ml) significantly induced contraction as a measure of wound healing activity (Fig. 2D). When compared to the activities of FGF2 (0.3 µg/ml), the contraction activity of SR-0379 (30 µg/ml) was more potent, while the other activities were equivalent or less potent in SR-0379. Interestingly, the treatment with SR-0379 significantly increased the mRNA expression of interleukin-8 (IL-8) which was attenuated with pretreatment of Wortmannin (PI3kinase inhibitor, 100 nM) (Figure S3A in File S1). Similarly, the treatment with SR-0379 increased IL-8 protein expression in a dose dependent manner Figure S3B in File S1).

What are the molecular mechanisms of these actions of SR-0379? The phosphorylation effects of SR-0379 on FAK at Tyr397 and Tyr925 and on Akt at Ser473 were examined in NHDFs. As shown in Fig. 3A, treatment with SR-0379 (10 µg/ml) increased the phosphorylation of FAK Tyr397 and Akt Ser473 but not of FAK Tyr925 after 30 minutes, similar to the well-known antimicrobial peptide LL-37. The treatment with SR-0379 at doses of 0.3 to 10 µg/ml also significantly increased the phosphorylation of FAK Tyr397 and Akt Ser473 (Fig. 3B). The involvement of integrins was also tested in NHDFs. Pretreatment with RGD peptide (30, 100 and 300 µM), a small-molecule integrin antagonist, inhibited the activation of FAK and Akt induced by SR-0379 (Fig. 3C). Wortmannin (100 nM) and Rapamycin (1 nM) also inhibited the activation of Akt induced by SR-0379 (Fig. 3D, 3E). The treatment with SR-0379 (10 µg/ml) resulted in a significant increase in cell proliferation of fibroblast, whereas Akt knockdown using siRNA attenuated SR-0379-induced cell proliferation (Figure 3F and Figure S4A in File S1). Similarly, an inhibitor of Akt by Akt inhibitor IV (1 µM) also attenuated SR-0379-induced cell proliferation (Figure S4B in File S1). These results demonstrated the importance of Akt pathway in the effect of SR-0379.



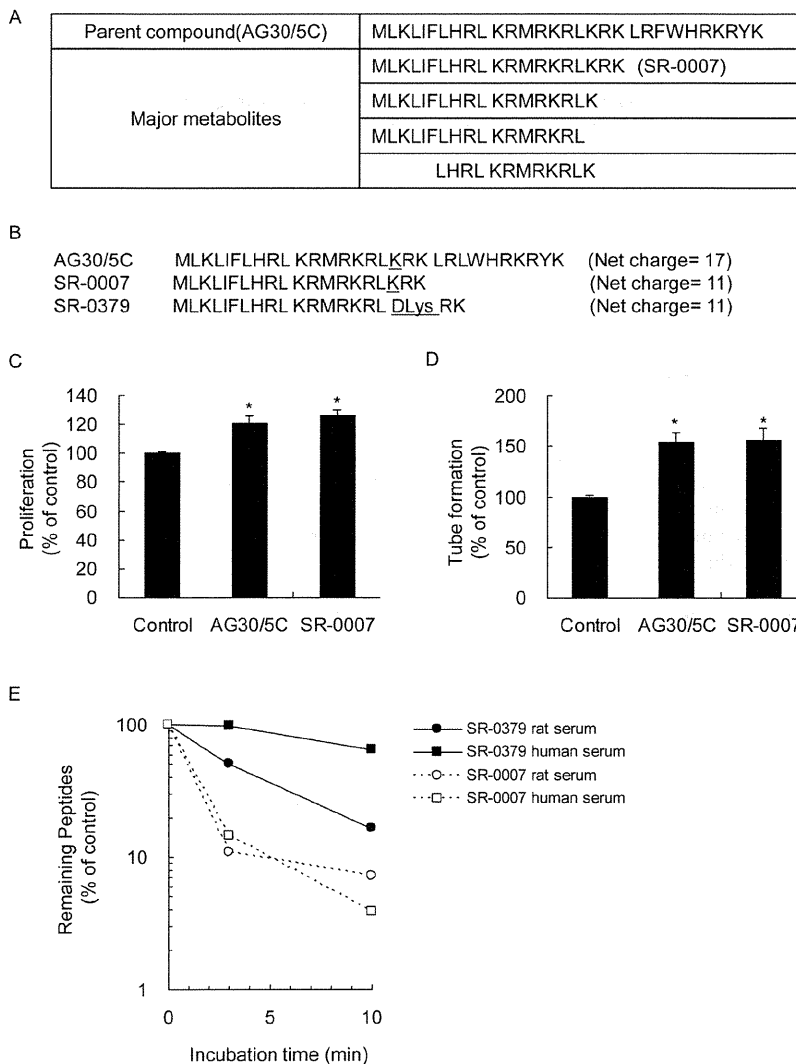


**Figure 1. Lead optimization from the angiogenic peptide AG30/5C.** A) Major metabolites of AG30/5C determined by MALDI-TOF MS. The parent compound (AG30/5C) was incubated with rat serum *in vitro* 60 minutes. The metabolites were identified by comparison with the pre-incubation peptide. B) Sequences and net charges of AG30/5C and AG30/5C-derived peptides (SR-0007 and SR-0379). The lysine (K) of SR-007 was replaced with D-lysine in SR-0379. C) Effect of AG30/5C (10 µg/ml) and SR-0007 (10 µg/ml) on HUVECs proliferation. N= 3 per group. \*P<0.05 vs. control. D) Effect of AG30/5C (10 µg/ml) and SR-0007 (10 µg/ml) on tube formation. The formation of capillary-like structures was observed in co-cultures of HUVECs and NHDFs. N=5-12 per group. \*P<0.05 vs. control. E) Stability of SR-0007 and SR-0379 in rat and human sera. SR-0007 and SR-0379 were quantified before or after incubation *in vitro* with rat and human sera for either 3 or 10 minutes. N=2. doi:10.1371/journal.pone.0092597.g001

### Acceleration of wound healing by SR-0379 *in vivo*

To evaluate the potential use of SR-0379 in clinical practice, a full-thickness wound model with a skin flap was employed in a streptozotocin-induced diabetic rat model. On day 2, the wound area was quickly and significantly reduced in the SR-0379 (0.2 mg/ml) group but not in the saline and FGF2 groups (Fig. 4A, 4B). As shown in Fig. 4A, the color of the wound surface on day 6 was red (bloody) in the SR-0379 treatment group. In contrast, the color of the wound surface was still dark with necrotic skin visible in both the saline and FGF2 groups. Reduced wound area in the SR-0379 group was sustained on days 6 and 13 (Fig. 4B). The skin wound was completely healed at day 19 with SR-0379 treatment, whereas the wound did not heal until day 24 with saline treatment (Fig. 4C).

To determine the utility of SR-0379 in a clinical situation, we finally evaluated whether the compound could accelerate wound healing in an acute infection wound model, as the presence of infection largely diminishes the wound-healing process. After creating full-thickness defects, *S. aureus* was inoculated. Treatment with SR-0379 (1 mg/ml) significantly reduced the unhealed wound size on days 8 and 15 compared to the saline and FGF2 groups (Fig. 5A, 5B). The effects of SR-0379 on wound healing were more potent than the effects of FGF2, which is currently a standard therapy (Fig. 4B, 5B). To determine the effect of SR-0379 on wound healing, granulation tissue formation was analyzed by subcutaneously implanting a paper disc (Fig. 5C). Granulation tissue weight was significantly increased by treatment with SR-0379 (100 µg/disc). To further evaluate the effect of SR-0379 on

**Table 1.** MICs of several compounds against *E. coli*, *P. aeruginosa* and *S. aureus*.

Compound	<i>E. coli</i> (ATCC25922)	<i>P. aeruginosa</i> (ATCC27853)	<i>S. aureus</i> (ATCC29213)
	MIC ( $\mu\text{g/ml}$ )		
AG30/5C	32	16/32	16/32
SR-0007	64	16/32	16/32
SR-0379	8	16/32	16
Tobramycin	0.25–1	0.25–1	0.12–1
Meropenem	0.008–0.06	0.25–1	0.03–0.12
Oxacillin	-	-	0.12–0.5

The scores indicate the MICs (mg/ml) for *E. coli*, *P. aeruginosa* and *S. aureus*. MICs represent the individual data from two independent experiments.  
doi:10.1371/journal.pone.0092597.t001

wound healing, collagen production and proliferation were measured using the incised wound rat model. The tensile strength after SR-0379 treatment (5  $\mu\text{g}$ ) was significantly increased compared to saline treatment. Treatment with SR-0379 induced granulation tissue formation and collagen production, which may accelerate wound healing.

Collagen gel assay is a conventional method to investigate cell behavior that more closely resembles cell behavior *in vivo*. As shown in Figure 2D, the diameter of the collagen gel containing went down by treatment of SR-0379. The promotion of the wound healing with SR-0379 was supported by the enhanced contraction *in vitro*.

## Discussion

Recently, wet dressing has been strongly recommended to accelerate the process of wound healing because epithelial cells and dermal fibroblasts proliferate well under wet conditions [13]. However, wounds under wet conditions present an ideal

environment for bacterial growth due to the presence of moisture and warmth. Wound infection has become one of the major risk factors in the delay of wound healing [14], although physicians take many precautions to prevent wound infection. Wound colonization is defined as the presence of multiplying microorganisms on the surface of a wound but with no associated clinical signs and symptoms of infection [15]. Recently, the term critical colonization has gained acceptance and is defined as the borderline of colonization and infection. As wound colonization is most frequently polymicrobial and involves numerous microorganisms that are potentially pathogenic, the diagnosis of clinical colonization is difficult for general physicians in a clinical setting. Recombinant growth factor proteins, such as FGF2 and PDGF, have been shown to stimulate ulcer-healing processes in clinical applications [16,17]. However, the wound might fail to be healed by these growth factors in the event of an infection, as these growth factors have no antibacterial properties. Therefore, a wound-healing drug with antibacterial properties would be ideal to avoid the risk of infection during wound care.

**Table 2.** *In vitro* activities of SR-0379 against Gram-positive and Gram-negative bacteria and fungi.

	Gram staining	Strain	MIC ( $\mu\text{g/ml}$ )		
			SR-0379	Chloramphenicol	
Bacteria	Aerobes	G(+)Bacilli	<i>Micrococcus luteus</i>	2	1
			<i>Bacillus subtilis</i>	2	4
		G(-)Bacilli	<i>Salmonella</i> Enteritidis	8	4
	<i>Salmonella</i> Typhimurium		8	4	
	<i>Acinetobacter baumannii</i>		8	16/32	
	Anaerobes	G(-)Bacilli	<i>Propionibacterium acnes</i>	16/32	NT
<i>Bacteroides fragilis</i>			32	1	
<i>Fusobacterium nucleatum</i>			16/32	0.25	
Fungi		Strain	SR-0379	Amphotericin B	
		<i>Penicillium glabrum</i>	8/16	0.125	
		<i>Fusarium solani</i>	8	1	
		<i>Alternaria alternata</i>	32	1	
		<i>Trichophyton mentagrophytes</i>	32	0.125	
		<i>Trichophyton rubrum</i>	64	0.125	
<i>Candida krusei</i>	32	2			

The scores indicate the MICs (mg/ml) for gram-positive and gram-negative bacteria and fungi. MICs represent the individual data from two independent experiments.  
NT: Not tested.

doi:10.1371/journal.pone.0092597.t002



**Table 3.** *In vitro* activities of SR-0379 against seven strains of drug-resistant bacteria.

Bacteria	Drug resistance	MIC (µg/ml)
<i>Pseudomonas aeruginosa</i>	Aminoglycoside-resistant	16
	Carbapenem-resistant	16–64
	Fluoroquinolone-resistant	16/64
<i>Staphylococcus aureus</i>	Methicillin-sensitive	32
	Methicillin-resistant (1)	32
	Methicillin-resistant (2)	32
<i>Acinetobacter baumannii</i>	Multidrug-resistant	16

MICs represent the individual data from two independent experiments.  
doi:10.1371/journal.pone.0092597.t003

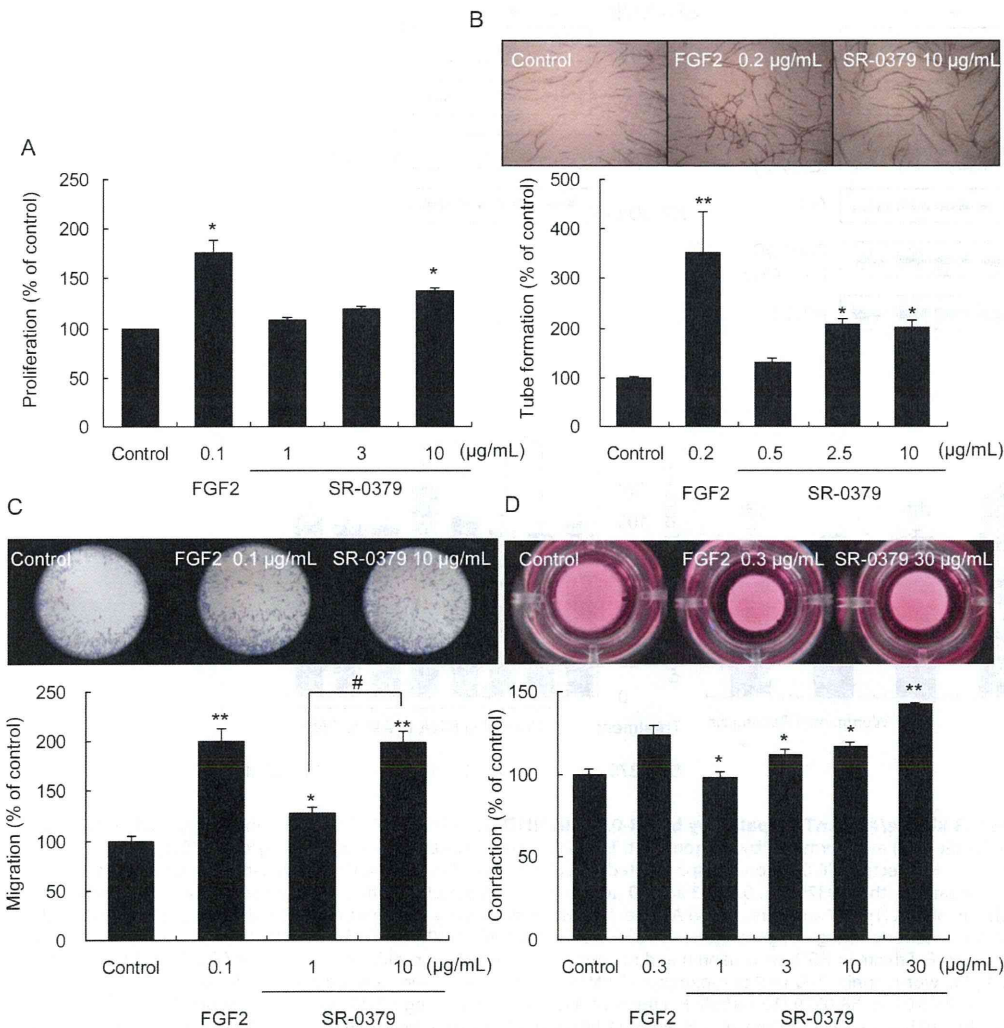


**Figure 2. Cellular function of SR-0379.** A) Effect of SR-0379 on NHDFs proliferation. NHDFs were treated with SR-0379 (1, 3 and 10 µg/ml) or FGF2 (0.1 µg/ml). N = 4 per group. \*P < 0.05 vs. control. B) The upper panel shows representative pictures of tube formation in a co-culture of HUVECs and NHDFs (Control, FGF2: 0.2 µg/ml) and SR-0379 (10 µg/ml). The lower panel shows the effects of SR-0379 on tube formation in a co-culture of HUVECs and NHDFs. N = 5 per group. \*P < 0.05, \*\*P < 0.01 vs. control. C) The upper panel shows representative pictures of the migration induced by FGF2 (0.1 µg/ml) and SR-0379 (10 µg/ml). The lower panel shows the effects of FGF2 (0.1 µg/ml) and SR-0379 (1 and 10 µg/ml) on migration. N = 4 per group. \*P < 0.05, \*\*P < 0.01 vs. control, #P < 0.01 vs. SR-0379 (1 µg/ml). D) The upper panel shows representative pictures of the fibroblast-collagen-matrix contraction assay with FGF2 (0.3 µg/ml) and SR-0379 (1, 3, 10 and 30 µg/ml). The lower panel shows the effects of FGF2 (0.3 µg/ml) and SR-0379 (1, 3, 10 and 30 µg/ml) on fibroblast-collagen matrix contraction. N = 3 per group. \*P < 0.05, \*\*P < 0.01 vs. control.  
doi:10.1371/journal.pone.0092597.g002

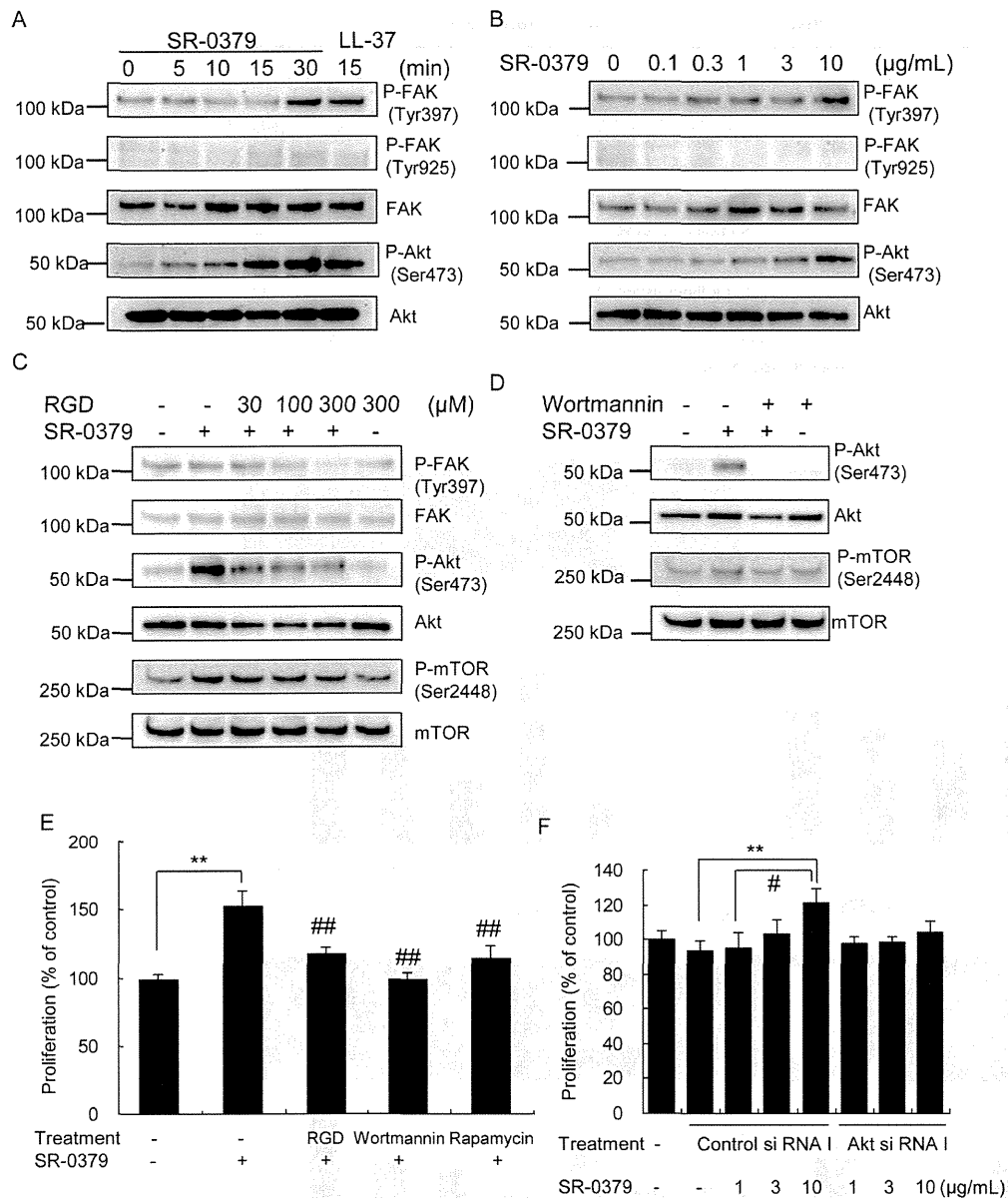


**Figure 3. Activation of the PI3 kinase/AKT/mTOR pathway by SR-0379 in NHDFs.** A) Effects of SR-0379 on phosphorylated FAK (Tyr397 and Tyr925) and phosphorylated Akt (Ser473) as determined by Western blot. The cells were treated with SR-0379 (10 µg/ml) for 0, 5, 15 and 30 minutes or LL-37 (10 µg/ml) for 15 minutes. B) Effects of SR-0379 on phosphorylated FAK (Tyr397 and Tyr925) and phosphorylated Akt (Ser473) as determined by Western blot. The cells were treated with SR-0379 (0.1, 0.3, 1, 3 and 10 µg/ml) for 30 minutes. C, D) Effects of RGD peptide and wortmannin on the SR-0379-induced phosphorylation of FAK (Tyr397 and Tyr925) and Akt (Ser473) as determined by Western blot. The cells were preincubated with RGD peptide (30, 100 and 300 µM, an inhibitor of integrin-ligand interactions) (C) or wortmannin (100 nM) (D) for 30 minutes and were then treated with SR-0379 (10 µg/ml) for 30 minutes. E) Effects of RGD, wortmannin and rapamycin on the NHDFs proliferation stimulated by SR-0379. The cells were preincubated with RGD (1000 µM), wortmannin (100 nM) or rapamycin (1 nM) for 2 hours and then were treated with SR-0379 (10 µg/ml). N = 3 per group. \*\*P<0.01 vs. control, ## P<0.01 vs. SR-0379 (10 µg/ml). F) Effects of Akt knockdown using siRNA on the NHDFs proliferation stimulated by SR-0379. The cells were pretreated with Akt si RNA or Control si RNA for 24 hours and then were treated with SR-0379 (1, 3 and 10 µg/ml). N = 4 per group. \*\*P<0.01 vs. control si RNA, # P<0.05 vs. SR-0379 (1 µg/ml) treated with control siRNA. doi:10.1371/journal.pone.0092597.g003

Based on this idea, we developed AG30, an antibacterial peptide with angiogenic activity. Although our previous study demonstrated that AG30/5C is useful to in the treatment of ulcers [8,9], cost and stability are problems for clinical applications. Therefore, in this study, we modified AG30/5C as a lead

compound to achieve 1) more stability upon exposure to serum, 2) lower cost, 3) wider antibacterial activity and 4) rapid wound healing. The initial analysis using the metabolites of AG30/5C revealed that a core sequence of 20 aa (MLKLIFLHRLKRMRLKRRK; SR-0007) was enough to